



Repositorio Institucional de la Universidad Autónoma de Madrid

<https://repositorio.uam.es>

Esta es la **versión de autor** del artículo publicado en:

This is an **author produced version** of a paper published in:

IEEE Transactions on Nanotechnology 8.2 (2009): 148 – 152

DOI: <http://dx.doi.org/10.1109/TNANO.2008.2009356>

Copyright: © 2009 IEEE

El acceso a la versión del editor puede requerir la suscripción del recurso

Access to the published version may require subscription

Contrast and Resolution of Nanowires in Electrostatic Force Microscopy

Gómez-Moñivas Sacha

Abstract - A detailed analysis of the contrast and lateral resolution between a dc-biased tip and metallic nanowires over a dielectric sample is presented. The theoretical technique used to analyze the interaction intrinsically includes the mutual polarization between the tip, the sample, and the metallic objects. A good selection of the dielectric constant of the sample is found to be critical since it can increase the contrast by more than an order of magnitude. On the other side, the dielectric constant does not have any influence on the lateral resolution. In this case, the tip-sample distance and the tip radius are the most relevant parameters. For small tip-sample distances, the length of the nanowires must also be taken into account since it can produce differences of up to 20% in the lateral resolution.

Index Terms – Atomic Force Microscopy, Electrostatic Forces, Nanowires.

I. INTRODUCTION

Electrostatic Force Microscopy (EFM) and its various implementations [1], [2] are based on the electrostatic interaction between a biased *Atomic Force Microscope* (AFM) [3] tip and a sample. Its high resolution and versatility have been used to analyze several properties of solid surfaces at the nanoscale [4], [5], [6], [7], [8], [9], to induce nanometric modifications on the surfaces [10], [11] or to obtain the dielectric response of single nanowires [12], [13]. Single nanowires can be used to connect different parts of a circuit in nanoelectromechanical systems (NEMS) [14] and will play an important role in future electronics [15], [16].

When EFM is working at the nanoscale, a large number of interacting parameters have a strong influence in the signal. However, Since EFM is a nonlocal technique due to the long-range nature of the electrostatic interaction, there is no simple way to directly relate the electrostatic images with the microscope setup [17] or the dielectric and topographic properties of the sample [18].

Most of the previous studies have focused on the interaction between metallic tips and metallic flat surfaces [19]. Some experiments on carbon nanotubes have also been compared with numerical methods [20]. In this paper we present a theoretical analysis of the lateral resolution and contrast of metallic nanowires in EFM. We will analyze the influence of several parameters with the objective of creating a reference

for experimentalists that are interested in improving the microscope performance. First we will develop a numerical method that takes into account all the mutual polarization terms between tip and nanowires. Applying the method to analyze the influence of the dielectric constant, we will show that, using a carefully selected sample, the contrast of the image can be increased over an order of magnitude. Furthermore, we will analyze the influence of the length of the nanowire in the lateral resolution. As we will demonstrate, the length of the nanotube has a strong influence in the lateral resolution when the tip-sample distance is much smaller than the tip radius.

II. ELECTROSTATIC FIELD CALCULATION

The geometry and parameters used in the calculations are sketched in Fig. 1. The tip is assumed to be a sphere of radius R_{tip} and voltage V_0 . The nanowires are modelled as perfect metallic cylinders with length L_T and radius R_T . The nanowires can be connected to an independent electrode at voltage V_T . The sample is semiinfinite with a uniform relative dielectric constant ϵ . The different elements of the system are related by the distance between nanowires h and the tip-sample distance D .

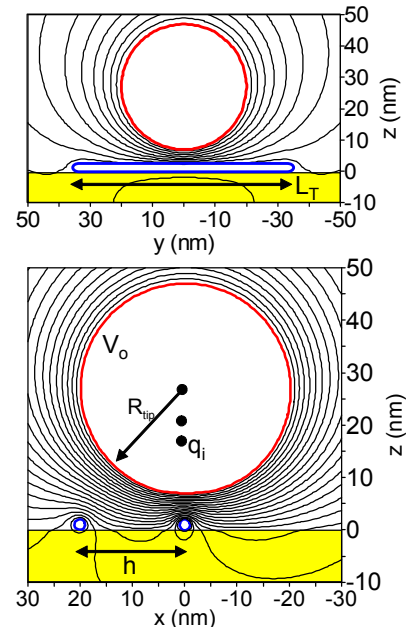


Figure 1: Electrostatic potential distribution calculated by the Generalized Image Charge Method for a spherical tip scanning over a sample composed by two grounded metallic nanowires over a dielectric sample.

Manuscript received August 1, 2008

G. M. Sacha is with the Department of Informatics, Escuela Politécnica Superior, Universidad Autónoma de Madrid, Cantoblanco, Madrid, Spain. Copyright (c) 2008 IEEE. Personal use of this material is permitted. However, permission to use this material for any other other purposes must be obtained from the IEEE by sending a request to pubs-permissions@ieee.org.

To reproduce the boundary conditions of a constant potential at the metallic surfaces of tip and sample, we use the Generalized Image Charge Method (GICM) [21]. The main details of the GICM have been described elsewhere [22] and therefore only a brief description is given here. The GICM generalizes the image charge method with the replacement of the tip by a set of punctual charges that are adjusted in order to keep constant the electrostatic potential over the tip surface. Plane surfaces, such as the sample or the cantilever [17], can be included in the simulation by a series of image charges [23].

The electrostatic force (and force gradient) can be obtained directly from the interaction of the charges inside the tip with their images or from the derivative of the capacitance C with respect to the tip-sample distance: $F=(V_0^2/2)(dC/dD)$.

In the modification of the GICM suggested here, the surface charge density of both tip and nanowires is substituted by a set of charge elements. This approximation is adequate when the nanotubes are metallic and the amount of free charge inside them is enough to fully compensate the external electric field. That condition is true in the case shown in this article (grounded nanotubes) since they can obtain a theoretically infinite amount of free charge from the electrodes. Assuming N punctual charges inside the tip and M linear charges inside the Q nanowires, the total potential at a point r would be

$$V(r) = \frac{1}{\epsilon_0} \sum_i^N q_i G(r, r_i) + \sum_q^Q \left[\sum_i^M \lambda_i G(r, r_i; \tilde{L}_i) \right] \quad (1)$$

where q_i and λ_i are the values of the charges inside the tip and the nanotubes respectively. L_i are the lengths of the segments inside the nanotubes. G is the potential (Green's function) generated by a charge/segment inside a parallel plate capacitor and can be divided into two contributions: $G=G_0+G_{\text{resp}}$. G_0 is the potential generated by the charge/segment itself and G_{resp} includes the contribution of the induced charges. Although G_0 has an analytical expression in most of the cases, G_{resp} will be an infinite series of image charges that must be calculated numerically. The values of q_i and λ_i are obtained after a standard least squares minimization of

$$\chi^2 = \sum_j^P (V(r) - V_0)^2 + \sum_j^T (V(r) - V_T)^2 \quad (2)$$

where P and T are the points generated at the tip and nanotube surfaces. It is worth noting that, due to the simultaneous fit of the potential in tip and nanowires, their mutual polarization is intrinsically included in the result. In Fig. 1, we show the equipotential distribution of a spherical tip over two metallic nanowires ($L_T=70\text{nm}$, $R_T=1\text{nm}$). Several publications show methods that can be combined with the one shown in this article. A similar technique, also inspired in the standard image charge method that includes arbitrary surfaces has been proposed by Lyuksyutov et al [24]. Arbitrary tip shapes can be

also included following the generalization of the GICM shown in [22].

III. CONTRAST OF SINGLE NANOWIRES

In this section we analyze the vertical gradient force F' obtained from a single grounded metallic nanowire over a dielectric sample. In Fig. 2, we show F' for a perpendicular scan over a metallic nanowire at different tip-sample distances (the nanowire is placed at $x=0$). Fig. 2a shows F' for a nanowire with no surface below ($\epsilon=1$) and Fig. 2b a nanowire over a metallic surface ($\epsilon=100$). In the first limit ($\epsilon=1$), $F'(x=0)$ decreases when D increases due to the higher distance between the charges of the tip and nanowire. On the other side, $F'(x \rightarrow \infty)$ vanishes because there is not any charge in the surface that can interact with the tip. Defining the contrast $\Delta F' = F'(x=0) - F'(x \rightarrow \infty)$, it is clear that $\Delta F'(\epsilon=1)$ is higher for small tip-sample distances. On the upper limit ($\epsilon=100$), we observe a similar behaviour when $x=0$. However, $F'(x \rightarrow \infty)$ tends to the gradient force between a metallic tip over a flat metallic sample ($F'(x \rightarrow \infty)$ can be approximated by $F'/\pi\epsilon_0 V^2 = R/D^2$ when $R>D$) [25]. Although both limits decrease when D increases, $\Delta F'(\epsilon=100)$ also vanishes when $D \rightarrow \infty$ since $F'(x=0)$ decreases faster.

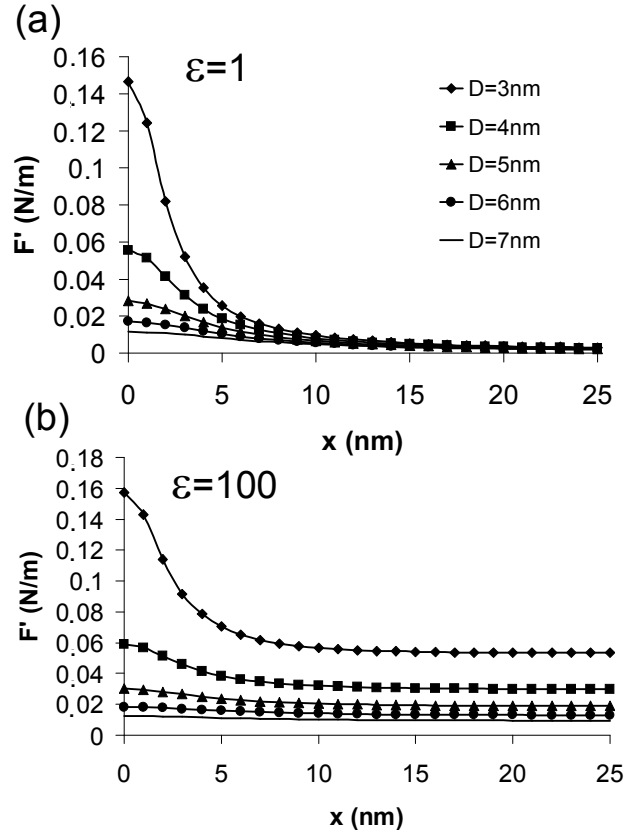


Figure 2: Vertical gradient force for a scan perpendicular to a metallic grounded nanowire. Results are shown for a nanowire with no surface below ($\epsilon=1$) and a nanowire placed on a metallic sample ($\epsilon=100$)

In figure 3a we analyze $\Delta F'$ for different values of D and ϵ . For all the ϵ values, we observe a strong decreasing of $\Delta F'$ when D increases that correlates with the information obtained in Fig.2. Moreover, higher values of ϵ also reduce $\Delta F'$. The origin of this effect is related to the value of the electrostatic potential in the dielectric surface $V(z=0)$. Higher ϵ values induce lower $V(z=0)$ (In the limit $\epsilon \rightarrow \infty$, the sample is metallic and $V(z=0)=0$). Assuming that the nanotubes are grounded, the electrostatic potential V_T on their surface should be zero. Being the nanotubes placed over the surface, the charge needed to keep $V_T=0$ can be considered proportional to $V(z=0)-V_T$ as a first approximation. Higher values of ϵ imply smaller amount of charge inside the nanotube and, as a direct consequence, smaller contrast. A direct conclusion would be that, although the electrostatic signal is higher with metallic samples, dielectric samples are desirable since $\Delta F'$ is higher for grounded metallic objects. To analyze the magnitude of this effect, we show in Fig. 3b the proportion $\Delta F'(\epsilon=1)/\Delta F'(\epsilon=100)$ for different tip-sample distances. For $D \approx R/4 \approx 5\text{nm}$ the proportion is around 2. However, when $D \approx R \approx 20\text{nm}$, $\Delta F'(\epsilon=100)$ is 12 times smaller than $\Delta F'(\epsilon=1)$. In this case, it is critical to use dielectric samples to obtain a good electrostatic contrast of the nanowires.

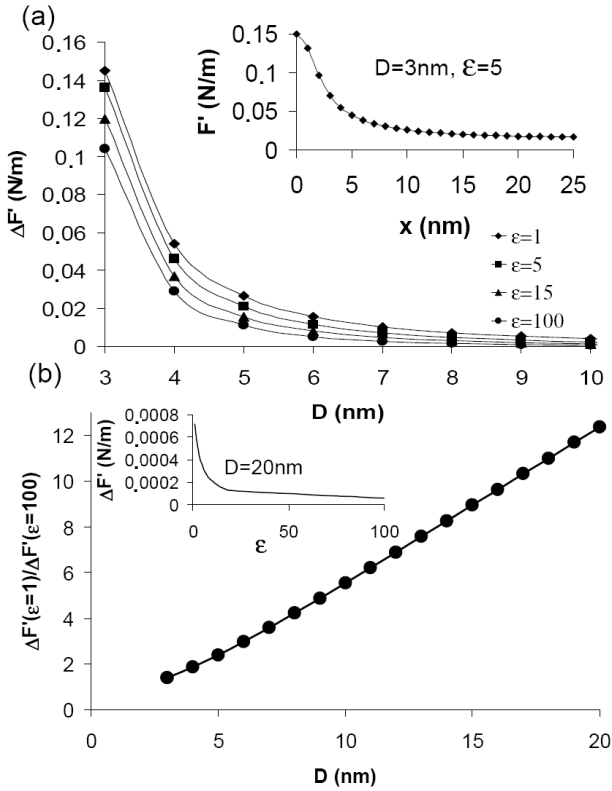


Figure 3: (a) Electrostatic contrast $\Delta F'$ for different tip-sample distances D and dielectric constants ϵ . Inset shows the gradient force curve that was used to obtain $\Delta F'$ for $D=3\text{nm}$ and $\epsilon=5$. (b) Coefficient between $\Delta F'(\epsilon=1)$ and $\Delta F'(\epsilon=100)$ vs D . Inset shows the contrast curve that was used to obtain the coefficient for $D=20\text{nm}$.

IV. LATERAL RESOLUTION

In this section we analyze the influence of the EFM parameters in the lateral resolution ΔX . In previous works [18], the electrostatic signal has been considered the convolution of two magnitudes: the equivalent surface profile and the response function. Following this approach [26], ΔX has been defined as the half width at half maximum of the response function. This definition is only accurate for very small objects since it comes from the approximation of the equivalent surface profile as a Delta function. To be sure that ΔX is well-defined, we obtain the resolution directly from the microscope signal.

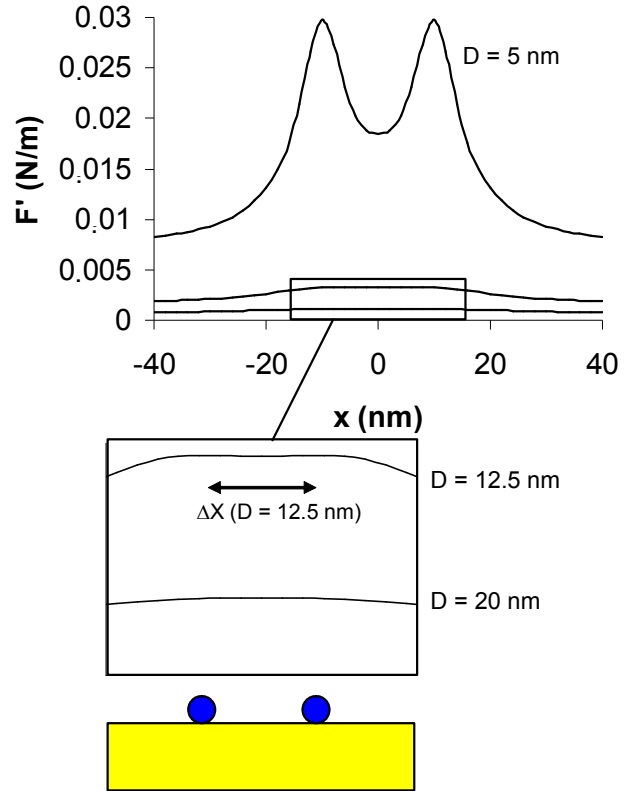


Figure 4: Vertical gradient force for a sample composed by two metallic nanowires placed at $x=\pm 10\text{nm}$ over a dielectric sample ($\epsilon=5$). An example of the criteria used in this work to define the lateral resolution can be shown in the enlarged representation at the bottom of the figure. $R_{\text{tip}}=20\text{nm}$, $L_T=70\text{nm}$, $R_T=1\text{nm}$ and $V_0=1\text{V}$.

In figure 4 we show F' for two metallic nanowires with $h=20\text{nm}$ at three different tip-sample distances ($D=5, 12.5, 20\text{nm}$). For $D=5\text{nm}$ the signal has two maximums when the tip scans over the nanowires. In this case, it is clear that F' comes from two independent objects. Although the effect is much smaller, the two maximums persists for $D=12.5\text{nm}$ (see the enlarged version of the curve at the bottom of Fig. 4). For $D>12.5\text{nm}$, the two maximums are substituted by a single one between the nanowires and it is not possible to distinguish the origin of the signal since it could come from two nanowires or a single one at $x=0$. In this example, the

lateral resolution would be $\Delta X(D=12.5\text{nm})=20\text{nm}$. Generalizing, we can define ΔX as the minimum separation of two objects that produce two independent maximums in the signal. To obtain the lateral resolution for a given D and R_{tip} , the two nanotubes will be initially placed far from each other. Then the distance between the nanotubes will be reduced until the two peaks in the signal disappear. The last distance that gives two peaks in the signal will be defined as the lateral resolution for the given values of D and R_{tip} . It is worth noting that this definition does not take into account experimental noise. The values obtained in this article for ΔX are the lowest ones that can be reached in EFM measurements.

We have analyzed ΔX for $1 < \varepsilon < \infty$, $4 < D < 20$, $R_{\text{tip}}=10, 20$ and $1 < L_T < \infty$ (units are nm for D , R_{tip} and L_T). For the numerical simulations, $L_T=70\text{nm}$ and $\varepsilon=100$ were used to simulate the infinite values. In agreement with previous results [26], we found that the lateral resolution ΔX does not depend on ε for any value of D , R_{tip} and L_T .

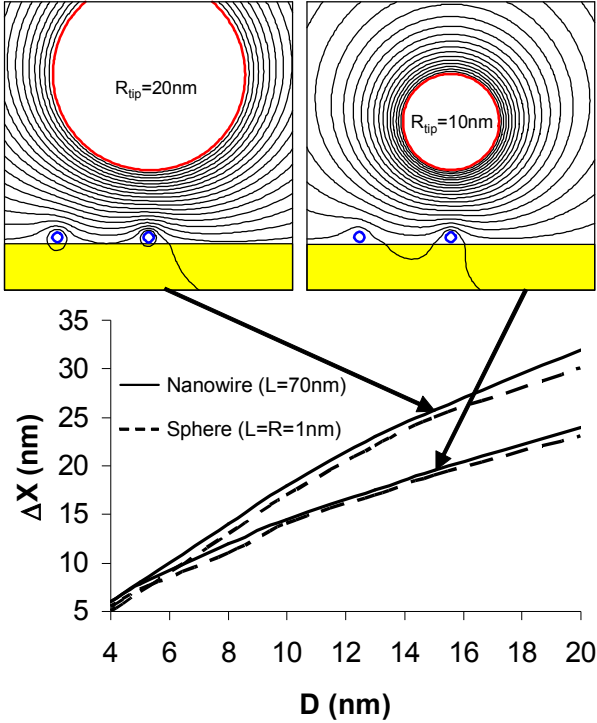


Figure 5: Lateral resolution for two different tips ($R_{\text{tip}}=10\text{nm}$ and $R_{\text{tip}}=20\text{nm}$) and two different objects (Nanowire $L_T=70\text{nm}$, $R_T=1\text{nm}$ and Sphere $L_T=R_T=1\text{nm}$). $V_0=1\text{V}$.

In figure 5 we show ΔX for two different tips ($R_{\text{tip}}=10\text{nm}$ and $R_{\text{tip}}=20\text{nm}$) and two different objects: spherical particles ($L_T=R_T=1\text{nm}$) and nanowires ($R_T=1\text{nm}$ and $L_T=70\text{nm}$). In analogy with other SPM techniques based on the electric field, ΔX is worse for higher values of D and R_{tip} . To explain this fact, we show in Fig. 5 equipotential distributions for $R_{\text{tip}}=10\text{nm}$ and $R_{\text{tip}}=20\text{nm}$. In these figures, we can see that the electric field penetrates easier between the nanowires when R_{tip} is smaller. For higher values of R_{tip} and D , the electrostatic

potential tends to be plane (perpendicular to the z axis) on the sample surface and cannot penetrate between the nanowires.

The influence of L_T is also analyzed in figure 5. The effect of L_T in the lateral resolution is surprisingly small. The difference ΔX_{dif} between $\Delta X(L_T=70\text{nm})$ and $\Delta X(L_T=1\text{nm})$ is almost constant for both $R_{\text{tip}}=10\text{nm}$ and $R_{\text{tip}}=20\text{nm}$ and never exceeds 2nm. The constant difference between both limits implies that the effect of L_T is higher for small tip-sample distances. We found $\Delta X_{\text{dif}}/\Delta X(L_T=1\text{nm}, R_{\text{tip}}=20\text{nm})=20\%$ and $\Delta X_{\text{dif}}/\Delta X(L_T=1\text{nm}, R_{\text{tip}}=10\text{nm})=10\%$ for $D=4\text{nm}$. However, for $D=20\text{nm}$, $\Delta X_{\text{dif}}/\Delta X(L_T=1\text{nm}, R_{\text{tip}}=20\text{nm})$ and $\Delta X_{\text{dif}}/\Delta X(L_T=1\text{nm}, R_{\text{tip}}=10\text{nm})$ never exceeds 7% and 4% respectively. For small tip-sample distances, water condensation can play an important role in both contrast and resolution when the AFM is working in a humid environment. The values of the distances [7], [8] that can induce a water bridge between tip and sample must be taking into account when both contrast and resolution are analyzed since the presence of water can drastically modify the electric field in that region.

V. CONCLUSIONS

We have presented a theoretical analysis of the contrast and lateral resolution in EFM. We have demonstrated that a good selection of the microscope setup parameters (dielectric constant of the reference sample and tip-sample distance) can increase the contrast by more than an order of magnitude. Depending on the tip-sample distance, the contrast of a single nanowire can be highly increased using dielectric samples instead of metallic ones. In particular, the contrast can be 12 times bigger for dielectric samples when $D \approx R_{\text{tip}}$. On the other side, the dielectric constant does not have any influence in the lateral resolution. The key parameters in this case are the tip-sample distance and the tip radius. Analyzing the properties of the sample, we have found a constant difference of 1-2nm in the lateral resolution between spherical particles and nanowires. Although the difference can be considered small, it reduces the lateral resolution by up to 20% when the tip-sample distance is small compared to the tip-radius.

ACKNOWLEDGMENT

Author acknowledges F. B. Rodríguez and P. Varona for insightful discussions. This work was supported by MEC TIN 2007-65989 and CAM S-SEM-0255-2006.

REFERENCES

- [1] J. Hu, X.-D. Xiao, and M. Salmeron, "Scanning polarization force microscopy: A technique for imaging liquids and weakly adsorbed layers," *Appl. Phys. Lett.*, vol. 67, pp. 476-478, 1995
- [2] A. N. Morozovska, E. A. Eliseev and S. V. Kalinin, "The piezoresponse force microscopy of surface layers and thin films: Effective response and resolution function," *J. Appl. Phys.*, vol. 102, pp. 074105(1)-074105(12), 2007

-
- [3] H. J. Butt, B. Capella and M. Kappl, "Force measurements with the atomic force microscope: Technique, interpretation and applications," *Surf. Sci. Rep.*, vol. 59, pp. 1-152, 2005
- [4] A. N. Morozovska, E. A. Eliseev, S. L. Bravina et al. "Resolution-function theory in piezoresponse force microscopy: Wall imaging, spectroscopy, and lateral resolution," *Physical Review B*, vol. 75, 174109(1)- 174109(18), 2007
- [5] E. Bonarcurso, F. Schonfeld and H. J. Butt, "Electrostatic forces acting on tip and cantilever in atomic force microscopy," *Phys. Rev. B.*, vol. 74, pp. 085413(1)- 085413(8), 2007
- [6] R. W. Stark, N. Naujoks and A. Stemmer, "Multifrequency electrostatic force microscopy in the repulsive regime," *Nanotechnology*, vol. 18, pp. 065502(1)- 065502(7), 2007
- [7] P. B. Paramonov and S. F. Lyuksyutov, "Density-functional description of water condensation in proximity of nanoscale asperity," *J. Chem. Phys.*, vol. 123, pp. 084705(1)-084705(7), 2005
- [8] G. M. Sacha, A. Verdaguer and M. Salmeron, "Induced water condensation and bridge formation by electric fields in Atomic Force Microscopy," *J. Phys. Chem. B.*, vol. 110, pp. 14870-14873, 2006
- [9] S. Gómez-Moñivas, J. J. Sáenz, M. Calleja and R. Garcia, "Field-Induced Formation of Nanometer-Sized Water Bridges," *Phys. Rev. Lett.*, vol. 91, pp. 056101(1)- 056101(4), 2003
- [10] S. F. Lyuksyutov, R. A. Vaia, P. B. Paramonov, S. Juhl, L. Waterhouse, R. M. Ralich, G. Sigalov and E. Sancaktar, "Electrostatic nanolithography in polymers using atomic force microscopy," *Nature Materials*, vol. 2, pp. 468-472, 2003
- [11] S. Juhl, D. Phillips, R. A. Vaia, S. F. Lyuksyutov and P. B. Paramonov, "Precise formation of nanoscopic dots on polystyrene film using z-lift electrostatic lithography," *Appl. Phys. Lett.*, vol. 85, p.p. 3836-3838, 2004
- [12] R. Quintero-Torres, "A Model for the Self Structuring of Nanotubes in Titanium Oxide," *IEEE Transactions on Nanotechnology*, vol. 7, pp. 371-375, 2008
- [13] T. S. Jespersen and J. Nygard, "Mapping of individual carbon nanotubes in polymer/nanotube composites using electrostatic force microscopy," *Appl. Phys. Lett.*, vol. 90, pp. 183108(1)- 183108(3), 2007
- [14] L. Dong, K. Shou, D. R. Frutiger, A. Subramanian, L. Zhang, B. J. Nelson, X. Tao and X. Zhang "Engineering Multiwalled Carbon Nanotubes Inside a Transmission Electron Microscope Using Nanorobotic Manipulation," *IEEE Transactions on Nanotechnology*, vol. 7, pp. 508-517, 2008
- [15] J. E. Jang, S. N. Cha, Y. Choi, D. J. Kang, D. G. Hasko, J. E. Jung, J. M. Kim, and G. A. J. Amaratunga, "A Nanogripper Employing Aligned Multiwall Carbon Nanotubes," *IEEE Transactions on Nanotechnology*, vol. 7, pp. 389-393, 2008
- [16] S. Pisana, C. Zhang, C. Ducati, S. Hofmann and John Robertson, "Enhanced Subthreshold Slopes in Large Diameter SingleWall Carbon Nanotube Field Effect transistors", *IEEE Transactions on Nanotechnology*, vol. 7, pp. 458-462, 2008
- [17] G. M. Sacha and J. J. Sáenz, "Cantilever effects on electrostatic force gradient microscopy," *Appl. Phys. Lett.*, vol. 85, pp. 2610-2612, 2004
- [18] S. Gómez-Moñivas, R. Carminati, J. J. Greffet and J. J. Sáenz, "Theory of electrostatic probe microscopy: A simple perturbative approach," *Appl. Phys. Lett.*, vol. 76, pp. 2955-2957, 2000
- [19] G. M. Sacha, A. Verdaguer, J. Martínez, J. J. Sáenz, F. Ogletree and M. Salmeron, "Effective tip radius in electrostatic force microscopy," *Appl. Phys. Lett.*, vol. 86, pp. 123101(1)-123101(3), 2005
- [20] W. Lu, D. Wang, and L. Chen, "Near-Static Dielectric Polarization of Individual Carbon Nanotubes," *Nanoletters*, vol. 7, pp. 2729-2733, 2007
- [21] G. M. Sacha, C. Gómez-Navarro, J. J. Sáenz and J. Gómez-Herrero, "Quantitative theory for the imaging of conducting objects in electrostatic force microscopy," *Appl. Phys. Lett.* vol. 89, pp. 173122(1)-173122(3), 2006
- [22] G. M. Sacha, E. Sahagún and J. J. Sáenz, "A Method for calculating capacitances and electrostatic forces in Atomic Force Microscopy," *J. Appl. Phys.*, vol. 101, pp. 024310(1)- 024310(4), 2007
- [23] W. R. Smythe, "Static and Dynamic Electricity," McGraw-Hill, New York, 1968
- [24] S. F. Lyuksyutov and P. B. Paramonov, "Induced nanoscale deformations in polymers using atomic force microscopy," *Phys. Rev. B.*, vol. 70, pp. 174110(1)-174110(8), 2004
- [25] S. Gómez-Moñivas, L. S. Froufe, A. J. Caamaño and J. J. Sáenz, "Electrostatic forces between sharp tips and metallic and dielectric samples" *Appl. Phys. Lett.*, vol. 79, pp. 4048-4050, 2001
- [26] S. Gómez-Monivas, L. S. Froufe, R. Carminati, J. J. Greffet and J. J. Sáenz, "Tip-shape effects on electrostatic force microscopy resolution," *Nanotechnology*, vol. 12, pp. 496-499, 2001

Gómez-Moñivas Sacha received the B.S. degree in Physics from Universidad Autónoma de Madrid, Madrid, Spain in 1999, the B. S. degree in Psychology from Universidad Nacional de Educación a Distancia, Madrid, Spain in 2003, and the Ph.D. in Physics from the Universidad Autónoma de Madrid, Madrid, Spain in 2003.

He was a Postdoctoral Fellow at the Lawrence Berkeley National Laboratory, Berkeley CA and the Nanoscience Technology Center, Orlando, FL. He is currently a researcher at the Department of Computer Science, Universidad Autónoma de Madrid. His current research interests include artificial neural networks, models of sensory systems and nanowires and their application to electronic devices.